JOURNAL OF VIROLOGY, Aug. 1998, p. 6838–6850 Vol. 72, No. 8
0022-538X/98/$04.00+0

Coronavirus Particle Assembly: Primary Structure Requirements of the Membrane Protein

CORNELIS A. M. DE HAAN,[1] LILI KUO,[2] PAUL S. MASTERS,[2] HARRY VENNEMA,[1] AND PETER J. M. ROTTIER[1]*

Institute of Virology, Department of Infectious Diseases and Immunology, Faculty of Veterinary Medicine, and Institute of Biomembranes, Utrecht University, 3584 CL Utrecht, The Netherlands,[1] and Wadsworth Center for Laboratories and Research, New York State Department of Health, Albany, New York 12201[2]

Received 23 December 1997/Accepted 17 May 1998

Coronavirus-like particles morphologically similar to normal virions are assembled when genes encoding the viral membrane proteins M and E are coexpressed in eukaryotic cells. Using this envelope assembly assay, we have studied the primary sequence requirements for particle formation of the mouse hepatitis virus (MHV) M protein, the major protein of the coronavirion membrane. Our results show that each of the different domains of the protein is important. Mutations (deletions, insertions, point mutations) in the luminal domain, the transmembrane domains, the amphiphilic domain, or the carboxy-terminal domain had effects on the assembly of M into enveloped particles. Strikingly, the extreme carboxy-terminal residue is crucial. Deletion of this single residue abolished particle assembly almost completely; most substitutions were strongly inhibitory. Site-directed mutations in the carboxy terminus of M were also incorporated into the MHV genome by targeted recombination. The results supported a critical role for this domain of M in viral assembly, although the M carboxy terminus was more tolerant of alteration in the complete virion than in virus-like particles, likely because of the stabilization of virions by additional intermolecular interactions. Interestingly, glycosylation of M appeared not essential for assembly. Mutations in the luminal domain that abolished the normal O glycosylation of the protein or created an N-glycosylated form had no effect. Mutant M proteins unable to form virus-like particles were found to inhibit the budding of assembly-competent M in a concentration-dependent manner. However, assembly-competent M was able to rescue assembly-incompetent M when the latter was present in low amounts. These observations support the existence of interactions between M molecules that are thought to be the driving force in coronavirus envelope assembly.

Enveloped viruses acquire their lipid envelopes by budding through cellular membranes. The viral envelope contains integral membrane proteins that play important roles in envelope formation and virus entry. Three models have been proposed for the budding of enveloped viruses. Two of these are based on nucleocapsid-dependent assembly. In retroviruses the nucleocapsid is all that is required, since the Gag core particle can direct its envelopment without the need for viral envelope proteins (9, 23, 31). In contrast, both core and spike proteins are essential for the formation of togaviruses (26, 71), envelopment being driven by direct interactions between the viral envelope proteins and the nucleocapsid (42, 78). In the case of rhabdoviruses, optimal budding efficiency and virus production are achieved by a concerted action of spike and internal virus proteins (48). In the third model, budding is nucleocapsid independent. Coexpression of flavivirus prM and E results in the formation of subviral particles resembling capsidless viral envelopes (1, 44). The hepatitis B virus (HBV) surface proteins can be independently secreted from cells as subviral particles, which, however, are morphologically quite distinct from HBV virions (58, 67). Recently we demonstrated that coronavirus envelope proteins have the capacity to assemble uniform envelopes, which have the same appearance and dimensions as virus particles, independently of nucleocapsid proteins (73).

Coronaviruses are positive-stranded RNA viruses with 30-kb genomes packaged in helical nucleocapsids. The nucleocapsid is incorporated into a viral particle by budding into the intermediate compartment between the endoplasmic reticulum (ER) and the Golgi complex (33, 35, 72). The coronavirus membrane contains three or four viral proteins. The membrane (M) glycoprotein is the most abundant structural protein; it spans the membrane bilayer three times, leaving a short NH_2-terminal domain outside the virus (or exposed luminally in intracellular membranes) and a long COOH terminus (cytoplasmic domain) inside the virion (reviewed by Rottier [62]). The spike protein (S) is a type I membrane glycoprotein that constitutes the peplomers. The small envelope protein (E) has been detected as a minor structural component in avian infectious bronchitis virus (IBV), transmissible gastroenteritis virus (TGEV), and mouse hepatitis virus (MHV) particles (reviewed by Siddell [66]), but it has not been extensively characterized. Some coronaviruses also contain a hemagglutinin-esterase protein (HE) (reviewed by Brian et al. [7]).

Molecular interactions between the envelope proteins are thought to determine the formation and composition of the coronaviral membrane. M plays a predominant role in the intracellular formation of virus particles, for which S appears not to be required. Growth of coronaviruses in the presence of tunicamycin gave rise to the production of spikeless, noninfectious virions (27, 51, 63, 69). These particles were devoid of S but contained M. Independently synthesized MHV M protein accumulates in the Golgi complex (33, 34, 65) in homomultimeric complexes (36). Heterotypic interactions between the M and S proteins have been identified by coimmunoprecipitation and sedimentation analyses (55). The S protein, on its own, is transported to the cell surface, but when it is associated with the M protein, it is retained in the Golgi complex. Upon co-

* Corresponding author. Mailing address: Institute of Virology, Faculty of Veterinary Medicine, Utrecht University, Yalelaan 1, P.O. Box 80.165, 3508 TD Utrecht, The Netherlands. Phone: 31-30-253246-2. Fax: 31-30-2536723. E-mail: P.Rottier@vetmic.dgk.ruu.nl.

TABLE 1. Primers used in site-directed mutagenesis

No.	Sequence	Resulting mutant[a]
1	5′-GTCTAAACATACACGGTACCTTTC-3′	
2	5′-CCAAACATTATGAATAGTAC-3′	S_2N
3	5′-AAGGTACCAAACATTATGGCTGCTAC	A_2A_3
4	5′-AAGGTACCAAACATTATGAGTAGTGCTGC-3′	A_4A_5
5	5′-CAAACATTATGAGTAGTACAACACAAGCCGCAGAGG-3′	A_8A_{10}
6	5′-CCAAACATTATGGCTAGTAG	Ains2
7	5′-CCAAACATTATGCATCACCATCACCATCACAGTAGCACTACTCAGGCCC-3′	His
9	5′-CACAGAATTCTGATTGGATCC-3′	
10	5′-GTGTATAGATATGAAAGGTACCGTG-3′	
11	5′-GCTCTAGACTACAATGCTGTGTCCGCGCC-3′	Δ3
12	5′-GCTCTAGATCACAACAATGCGGTGTCCG-3′	Δ2
13	5′-GCTCTAGACTATCTCAACAATGCGGTGTC-3′	Δ1
14	5′-CGTCTAGATTAGATTCTCAACAATGCGG-3′	$T_{228}I$
15	5′-CGTCTAGATTAGATTCTCAACAATGCGG-3′	$T_{228}L$
16	5′-GCTCTAGATTAGACTCTCAACAATGCGG-3′	$T_{228}V$
17	5′-GCTCTAGATTAGTTTCTCAACAATGCGG-3′	$T_{228}N$
18	5′-GCTCTAGATTAGATATTATTTCTCAACAATGCGG-3′	OC
19	5′-CGTCTAGATCCGGTTCTCAACAATG-3′	+5
20	5′-GCTCTAGATTAGGTTGCCAACAATGCGGTG-3′	$R_{227}A$
21	5′-TTAGGTGTCCGCGCCACTCGGT-3′	Δ5
22	5′-CTATTTGTTTGAGGGCAGTCGG-3′	Δ11
23	5′-TTAATTTCCGACCTTGGACTTC-3′	Δ18
24	5′-GTCCAAGGTAGGAAACGGCCGACTGC-3′	$Y_{211}G$
PM149	5′-GATTACCATACACTAACA-3′	
LK-10	5′-CAACAATGCGGTGTCCGCGCCAC-3′	
LK-24	5′-CGCATTGTTGAGA(GATC)T(GC)TAATCTAAAC-3′	$T_{228}M$, $T_{228}I$, $T_{228}L$, $T_{228}F$, $T_{228}V$
LK-26	5′-GATATGAAGGGTACCATGTATGTTAGGCCG-3′	
LK-27	5′-CATCCTTAAAGTTTAGATTAGATATTATTTCTC-3′	BCV
LK-28	5′-TAATCTAAACTTTAAGGATGTCTTTTGTTC-3′	BCV
LK-29	5′-GCGATTATTTGGCCCACGGG-3′	
LK-30	5′-CACCGCATTGTTGAGA(AT)A(GT)TAATCTAAACTTTAAGG-3′	$T_{228}Y$
LK-31	5′-CACCGCATTGTTGAGAAATTAATCTAAACTTTAAGG-3′	$T_{228}N$
LK-32	5′-CACCGCATTGTTGAGATAGTAATCTAAACTTTAAGG-3′	Δ1
LK-38	5′-ACCGCATTGTTGTAGACCTAATCTAAAC-3′	Δ2
LK-39	5′-AGATTAGGTCTACAACAATGCGGTGTCCGCGCC-3′	Δ2
LK-40	5′-GACACCTAGTAGTTGAGAACCTAATCTAAAC-3′	Δ5
LK-41	5′-GGTTCTCAACTACTAGGTGTCCGCGCCACTCGG-3′	Δ5
LK-42	5′-GGAAATTAATAGCGACTGCCCTCAAACAAACCG-3′	Δ18
LK-43	5′-GGGCAGTCGCTATTAATTTCCGACCTTGGACTTC-3′	Δ18

[a] Primers 1 to 24 were used for construction of expression vectors for VLP mutants. Primers PM149 to LK-43 were used for construction of transcription vectors for the generation of viral mutants.

expression of M, S, and E by using the vaccinia virus T7 system (20), virus-like particles (VLPs) containing these three viral membrane proteins were assembled in and released from cells. However, only M and E were required for particle formation. The S protein was dispensable but was incorporated when present (6, 73). The envelope particles produced by this system were shown to form a homogeneous population of spherical particles indistinguishable from authentic virions in size and shape (73).

One of our main interests is to understand the process of coronavirus assembly. We are particularly interested in the interactions and the mechanisms that drive the formation of the viral particles. With the VLP assembly system, we have developed an ideal tool for the study of coronavirus envelope formation and for the analysis of the interactions between the viral membrane proteins in molecular detail. In the present study, we have used the VLP assembly system to investigate the primary structure requirements of the M protein in envelope formation. Site-directed mutations in the carboxy terminus of M were also incorporated into the MHV genome by targeted recombination. The results demonstrate that particle assembly is critically sensitive to changes in all domains of the M molecule.

MATERIALS AND METHODS

Cells and viruses. Recombinant vaccinia virus encoding the T7 RNA polymerase (vTF7-3) (20) was obtained from B. Moss. OST7-1 cells (15) (obtained from B. Moss) were maintained as monolayer cultures in Dulbecco's modified Eagle's medium (DMEM) containing 10% fetal calf serum (FCS), 100 IU of penicillin/ml, 100 μg of streptomycin/ml, and 400 μg of G418/ml (all from Life Technologies, Ltd., Paisley, United Kingdom). Baby hamster kidney cells (BHK-21) obtained from the American Type Culture Collection (ATCC; Manassas, Va.) were maintained in the same medium lacking G418.

Expression vectors and transcription vectors. Expression construct pTM5ab contains the MHV open reading frames (ORFs) 5a and 5b, the latter encoding the E protein (73) in pTUG3 (74). Expression construct pTUMM contains the MHV strain A59 M gene (obtained from H. Niemann) cloned in the same vector as an *Xho*I fragment (73). The carboxy-terminal amino acid of the M protein coded by this clone is Thr (46, 54) rather than Ile, the terminal residue originally reported (2). A number of mutations were introduced into the M gene within this construct. Mutations in the amino-terminal domain (designated S_2N, A_2A_3, A_4A_5, A_8A_{10}, Ains2, and His) were made by PCR mutagenesis using 5′ terminal primers (Table 1, primers 2 through 7) directing the desired mutations and a 3′ internal primer (primer 1) corresponding to the region of the M gene that contains the unique *Kpn*I site. PCR fragments were first cloned into the pNOTA/T7 shuttle vector according to the Prime PCR Cloner procedure (5 Prime→3 Prime, Inc.) and were subsequently retrieved by cutting with *Kpn*I, after which the purified fragments were cloned into the expression vector pTUMM, from which the corresponding M fragment had been removed by using *Kpn*I. Mutants ΔN, ΔC and $G_{11}N_{13}$ were made by using single-stranded phagemid DNA according to the method of Zoller and Smith (79) as described previously (64). Mutant S_3N was made similarly by using primer 8. These mu-

tants were expressed from the transcription vector pTZ19R (47). For the construction of carboxy-terminal M mutants for VLP expression, an intermediate cloning vector was made as follows. By using a 5′ flanking primer (primer 9) and a 3′ terminal primer (primer 20), the M gene was prepared by PCR from a vector (pSFV1; Life Technologies, Inc.) containing the MHV M gene as a *Bam*HI fragment. The PCR fragment was cloned into the pNOTA/T7 shuttle vector. This vector was recleaved with *Bam*HI, and the resulting fragment was cloned into pBR322. The resulting cloning plasmid (pBMΔ5) contains the mutant M gene Δ5 as a *Bam*HI fragment and has a unique *Xba*I site flanking the 3′ terminus. The Δ3, Δ2, Δ1, T_{228}I, T_{228}L, T_{228}V, T_{228}N, OC, +5, and R_{227}A mutant M genes were all made by PCR mutagenesis using a 5′ internal primer (primer 10) containing the unique *Kpn*I site and a 3′ terminal primer containing the desired mutation and an *Xba*I site (primers 11 through 20). The PCR fragments were digested with *Kpn*I and *Xba*I and cloned into pBMΔ5 that had been treated with the same enzymes. The mutant M genes were finally cleaved out with *Bam*HI and cloned into expression vector pTUG3. Mutants Δ18, Δ11, and Δ5 were also made by PCR mutagenesis using a 5′ internal primer (primer 10) and 3′ terminal primers (primers 21 through 23), and the PCR fragments were cloned into pGEM-T (Promega). The plasmids were digested with *Kpn*I and *Spe*I, and the resulting fragments were cloned into expression vector pTUMM treated with *Kpn*I and *Xba*I. The Y_{211}G mutant was made with the Altered Sites site-directed mutagenesis kit purchased from Promega. The MHV M gene was cloned as a *Bam*HI fragment into pALTER-1. Primer 24 was used to introduce the mutations, and pALTER-1 was used as the expression vector.

For the construction of carboxy-terminal M mutants to be incorporated into the MHV genome, splicing overlap extension (SOE)-PCR was used as described previously (59) to create mutations in the transcription vector pCFS8 (16). This plasmid encodes a runoff transcript that contains a 5′ segment of the MHV genome fused to the entire 3′ end of the genome beginning with the S gene and is tagged with a 19-base substitution in gene 4 (16). PCR products containing the T_{228}M, T_{228}I, T_{228}L, T_{228}F, and T_{228}V mutations were generated by two rounds of PCR using inside primers LK-24 (which is partially degenerate) and LK-10 with external primers PM149 (upstream) and LK-29 (downstream). The same scheme was used to produce the T_{228}Y, T_{228}N, and Δ1 mutations, substituting primers LK-30, LK-31, and LK-32, respectively, for LK-24. Similarly, PCR products containing the Δ2, Δ5, and Δ18 mutations were generated with the inside primer sets LK-38 and LK-39 (Δ2), LK-40 and LK-41 (Δ5), and LK-42 and LK-43 (Δ18). Each PCR product was restricted with *Bss*HII and *Bsr*FI and was incorporated into the parent vector via a three-way ligation with the *Bsr*FI-*Nhe*I and *Bss*HII-*Nhe*I fragments of pCFS8. The T_{228}F mutant turned out to have a second, unintended mutation generating the substitution T_{223}I. For the construction of a chimeric mutant exchanging the carboxy-terminal half of the MHV M protein with that of bovine coronavirus (BCV), SOE-PCR was used to generate a perfect substitution bounded by the *Kpn*I site and the M-gene stop codon. In the first round of PCR, primers LK-26 and LK-27 were used to amplify the 3′ terminus of the BCV M gene from plasmid p(M+N)CAT1 (provided by David Brian), and primers LK-28 and LK-29 were used to amplify the downstream MHV region (the M-N intergenic junction and the 5′ end of the N gene) from pFV1 (16), which is identical to pCFS8 except that it does not contain the gene 4 tag. The second-round PCR product, obtained from primer pair LK-26 and LK-29 by using the first-round products as the template, was then restricted with *Kpn*I and *Bsr*FI and was ligated with the *Bsr*FI-*Nhe*I fragment of pCFS8 into an appropriate subclone. Finally, the fragment running from the *Eco*RV site at the end of gene 5 through the *Nhe*I site in the N gene was transferred from this intermediate to the vector pFV1. All PCR constructs were verified by sequencing.

Infection and transfection. Subconfluent monolayers of OST-7 and BHK-21 cells in 10-cm^2 tissue culture dishes were inoculated at 37°C with vTF7-3 in DMEM at a multiplicity of infection of 10. After 1 h (t = 1 h), cells were washed with DMEM and medium was replaced with transfection mixture, consisting of 0.2 ml of DMEM without FCS but containing 10 μl of Lipofectin (Life Technologies) and 5 μg of each selected construct. After 10 min at room temperature (RT), 0.8 ml of DMEM was added and incubation was continued at 37°C. At t = 2 h, cells were transferred to 32°C and incubation was continued.

Metabolic labeling and immunoprecipitation. At t = 4.5 h, cells were washed with phosphate-buffered saline (PBS) containing Ca^{2+} and Mg^{2+} (PBS^{++}) and were starved for 30 min in cysteine- and methionine-free MEM, containing 10 mM HEPES, pH 7.2, without FCS. The medium was then replaced by 600 μl of the same medium containing 100 μCi of ^{35}S in vitro cell labeling mix (Amersham). After 3 h, cells were placed on ice, and the media were collected and cleared by centrifugation for 15 min at 4,000 × g and 4°C. Cells were washed with ice-cold PBS^{++} and lysed with lysis buffer, consisting of 20 mM Tris-HCl (pH 7.6), 150 mM NaCl, 1% Nonidet P-40 (NP-40), 0.5% sodium deoxycholic acid (NaDOC), 0.1% sodium dodecyl sulfate (SDS), 2 μg of aprotinin/ml, 2 μg of leupeptin/ml, and 1 μg of pepstatin A/ml. Lysates were cleared by centrifugation for 10 min at 10,000 × g and 4°C. Radioimmunoprecipitation was performed on lysates diluted 5 times with immunoprecipitation buffer, consisting of 20 mM Tris-HCl (pH 7.6), 150 mM NaCl, 5 mM EDTA, 0.5% NP-40, 0.1% NaDOC, 0.1% SDS, and protease inhibitors. Culture media were prepared for immunoprecipitation by addition of 1/4 volume of 5-times-concentrated lysis buffer. Rabbit anti-MHV serum k134 (61) was used at a 500-fold dilution for immunoprecipitation of MHV proteins at 4°C. The immune complexes were adsorbed to Pansorbin cells (Calbiochem) for 30 min at 4°C and were subsequently collected by centrifugation. Pellets were washed three times by resuspension and centrifugation using 20 mM Tris-HCl (pH 7.6)–150 mM NaCl–5 mM EDTA–0.1% NP-40 followed by a single wash using 20 mM Tris-HCl (pH 7.6)–0.1% NP-40. The final pellets were suspended in electrophoresis sample buffer and heated at 95°C for 2 min before analysis by SDS-polyacrylamide gel electrophoresis (PAGE) using a 15% polyacrylamide gel according to the method of Laemmli (38). In some cases immunoprecipitates were digested with endoglycosidase F/*N*-glycosidase F (glyco F; Boehringer Mannheim) as described earlier (10) before analysis by SDS-PAGE.

Indirect immunofluorescence. Indirect immunofluorescence was performed on BHK-21 cells grown on 12-mm coverslips. The morphology of these cells makes them more convenient than OST7-1 cells for this assay. Cells were fixed at t = 5 h, permeabilized, and stained for immunofluorescence as described previously (33). The rabbit anti-MHV serum k134 was used at a 1:400 dilution.

Construction of MHV mutants. Carboxy-terminal M mutations were incorporated into the genome of MHV by targeted recombination between synthetic donor RNA from *Hin*dIII-truncated transcription vectors and the thermolabile N-gene deletion mutant Alb4 as described previously (16, 45, 59). Candidate recombinant viruses were plaque purified and analyzed by reverse transcription-PCR (RT-PCR) and sequencing of RNA from infected cells. Final confirmation of the construction of individual mutants came from direct sequencing of RNA isolated from purified virions (16, 59).

RESULTS

Effects of cytoplasmic-domain mutations on VLP assembly. In order to elucidate the primary structure requirements of the MHV M cytoplasmic domain for virus assembly, we constructed a number of mutants. Mutant ΔC has a large internal deletion, removing residues E_{121} through D_{195}, which comprise most of the amphiphilic domain. Mutant Δ18 lacks the carboxy-terminal hydrophilic domain. Since this deletion appeared to have a drastic effect on VLP assembly, a series of mutants was made with progressively smaller deletions at the carboxy terminus, ranging from 11 amino acids to a single amino acid (Fig. 1). The abilities of these mutant M molecules to function in assembly were tested by coexpressing each of the mutant genes with the E protein gene. Genes were expressed by using the recombinant vaccinia virus bacteriophage T7 RNA polymerase system in OST7-1 cells. Proteins were labeled with ^{35}S-labeled amino acids from 5 to 8 h postinfection. Cells and media were collected separately and processed for immunoprecipitation with a polyclonal rabbit anti-MHV serum, followed by SDS-PAGE using a 15% polyacrylamide gel. Analysis of the cell lysates (Fig. 2) of the single expressions demonstrated that all mutant constructs were expressed and yielded products of expected sizes. In all cases M appeared as a set of proteins differing in apparent molecular size, due to different extents of O glycosylation (34, 72). The patterns of the glycosylated species of M mutants were not much different from that of the wild-type (WT) M protein, indicating that the mutations in the carboxy terminus did not affect the ability of the amino terminus to become glycosylated, nor did they affect the ability of the proteins to be transported to the Golgi complex, as the slowest-migrating forms of M are known to result from modifications occurring in this organelle (34). Transport to the Golgi complex was confirmed by immunofluorescence analyses as illustrated in Fig. 3. The mutant M proteins were also analyzed for their stability by pulse-chase experiments and appeared to be as stable as WT M. In the double expressions, the presence of the E protein did not seem to affect the synthesis of M qualitatively under the experimental conditions used; in some cases, the expression level of M was somewhat decreased. The E protein itself was not resolved due to poor recognition by the antiserum, but its synthesis was confirmed by using an E-specific serum (data not shown). Particle assembly and secretion were assayed by measuring the release of the M protein into the culture medium. The E protein was extremely difficult to detect in VLPs, due to its small size and very

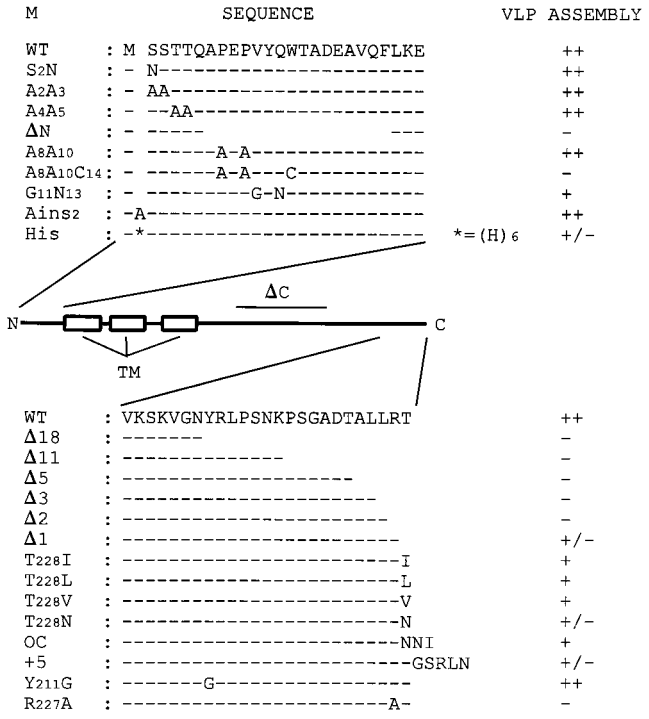

FIG. 1. Overview of mutant M proteins. In the middle is a schematic representation of the structure of the M protein, with the three transmembrane (TM) domains indicated. Amino acid sequences of the amino-terminal and carboxy-terminal domains, and of the mutants with mutations in these domains, are shown above and below the diagram, respectively. Dashes represent unchanged residues, gaps represent deletions. The domain deleted in mutant ΔC (residues E_{121} through D_{195}) is indicated by a horizontal line. The abilities of the different M proteins to support VLP assembly is indicated at the right. The ratio of the amount of M present in the culture medium to that in cells was taken as a measure for VLP assembly by using WT M as a reference. The semiquantitative scores ++, +, +/−, and − indicate efficient, moderately efficient, inefficient, and nonexistent VLP synthesis, respectively.

low abundance (73). It is clear from observation of WT M protein that no M was released into the medium unless the E protein was coexpressed, consistent with our earlier findings (73). However, all mutant M proteins failed to be secreted into the culture medium when they were expressed in combination with the E protein. Not only an internal deletion in the cytoplasmic domain but also deletions at the carboxy terminus were fatal for VLP assembly. Even the deletion of one single amino acid at the extreme carboxy terminus abolished VLP formation almost completely (Fig. 2), indicating that the carboxy-terminal residue is very important.

We therefore prepared a number of additional mutants with various changes at the very carboxy-terminal end. This second set of M mutants consisted of a panel of molecules in which the C-terminal threonine residue was replaced either by isoleucine (which is present at this position in a number of MHV strains [28]) or by leucine, valine, or asparagine. Furthermore, we prepared a mutant (OC) with a carboxy-terminal sequence identical to that of the human coronavirus (strain OC43) and BCV M proteins; a mutant with an extension of 5 foreign amino acids (+5); a mutant with a replacement of the Y at position 211 by G ($Y_{211}G$), which allows the protein to be detected at the cell surface (unpublished data); and a mutant in which R at position 227 was replaced by A ($R_{227}A$) (Fig. 1). These mutant constructs were expressed alone and in combination with the E protein gene. Cells and media were processed and analyzed as described above. The results (Fig. 4) showed that all mutants were expressed, producing proteins of the expected sizes. All M mutants again appeared as a set of differently glycosylated species not much different from that of WT M, indicating that they all had preserved the ability to become glycosylated and to be transported to the Golgi complex. When the appearance of the M protein in the culture medium is used as a measure for VLP assembly, it is clear that no M proteins were secreted during the single expressions. When the E protein was coexpressed, mutants $T_{228}I$, $T_{228}L$, $T_{228}V$, OC, and $Y_{211}G$ were released into the medium, although with decreased efficiency compared to WT. Mutants $T_{228}N$ and +5 almost completely failed to be secreted, while mutant $R_{227}A$ was not secreted at all. Quantitative analysis using a phosphorimager, taking the ratio of the amount of M present in the culture medium to that in cells as a measure of VLP assembly, showed that $T_{228}I$, $T_{228}L$, $T_{228}V$, OC, and $Y_{211}G$ had two- to fourfold reductions in VLP yield. For mutants $T_{228}N$ and +5, this decrease was 10- to 20-fold; the extension with 5 foreign amino acids was more detrimental for VLP assembly than replacement of the C-terminal residue by asparagine. These results demonstrate that VLP assembly is very sensitive to changes at the extreme C terminus. The tyrosine at position 211 does not seem to be important for VLP assembly (Fig. 4).

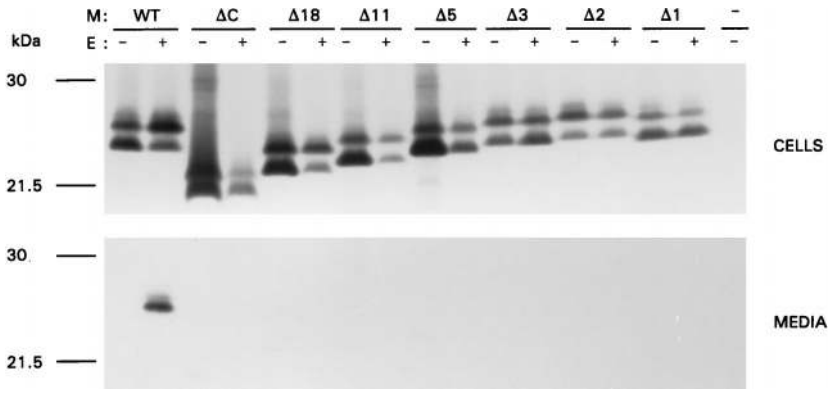

FIG. 2. Effects of deletions in the M cytoplasmic domain on VLP assembly. OST7-1 cells infected with recombinant vaccinia virus vTF7-3 were transfected with a plasmid containing the WT or mutant M gene either alone or in combination with a plasmid containing the E protein gene, each gene behind a T7 promoter. Cells were labeled for 3 h with ^{35}S-labeled amino acids. Both cells (upper panel) and the culture medium (lower panel) were prepared and used for immunoprecipitation, and the precipitates were analyzed by SDS-PAGE. The different M genes expressed are indicated above each set.

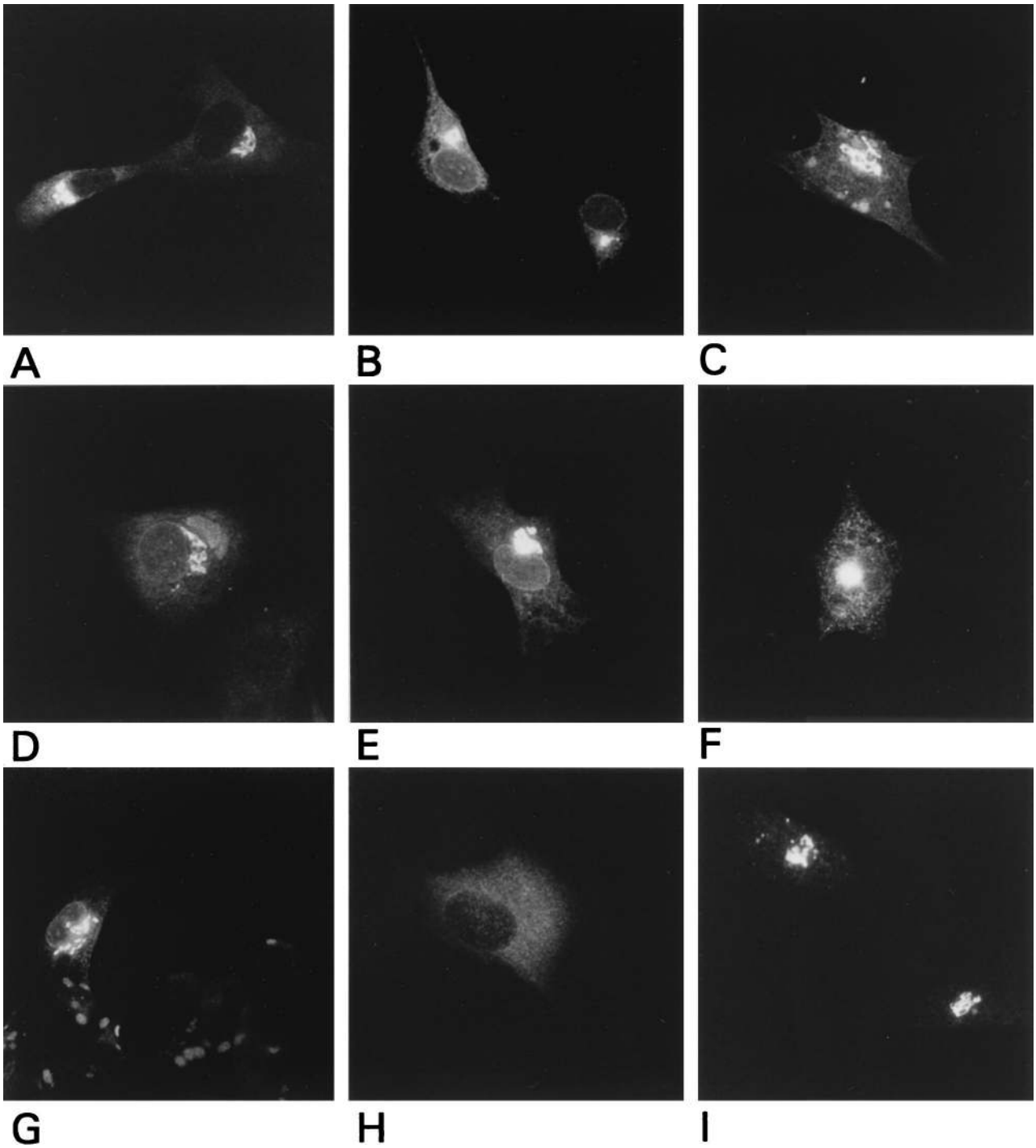

FIG. 3. Indirect immunofluorescence analysis of mutant M proteins. vTF7-3 infected BHK-21 cells were transfected with plasmids encoding WT M (A) or the ΔC (B), Δ18 (C), ΔN (D), A_4A_5 (E), A_8A_{10} (F), or $A_8A_{10}C_{14}$ (G) mutant or were mock transfected (H and I). Cells were fixed at 5 h postinfection and processed for immunofluorescence with the anti-MHV serum k134 (A through H) or a polyclonal rabbit serum against the resident Golgi protein α-mannosidase II (I) (a kind gift from K. Moremen [50]).

Effects of transmembrane deletions on VLP assembly. To assess the role of the transmembrane domains in VLP assembly, mutant proteins lacking either the first (Δa), the second (Δb), or the third (Δc) transmembrane domain or combinations thereof [Δ(a+b), Δ(b+c), and ΔaΔc] were tested for their VLP-forming abilities. The construction of these mutants and their expression in vitro and in vivo have been described earlier (37). When these mutant M proteins were coexpressed with E, no VLPs were detected in any case (data not shown). These results indicate the importance of the transmembrane domains in preserving the functional structure, orientation, and localization of the M molecule.

Effects of amino-terminal domain mutations on VLP assembly. Next, we wanted to investigate whether VLP formation is

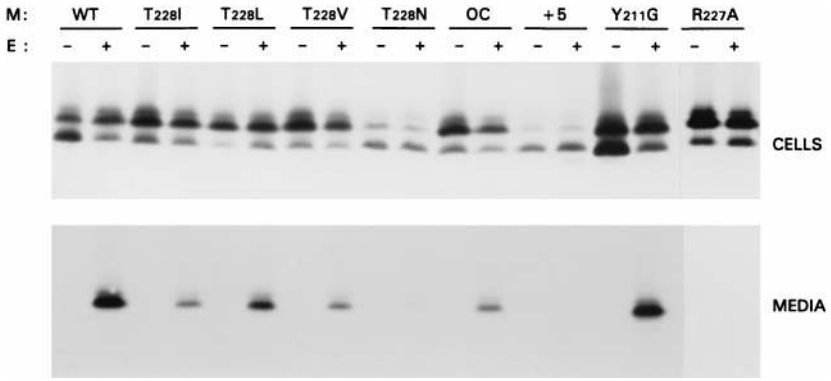

FIG. 4. Effects of mutations in the M carboxy-terminal domain on VLP assembly. Expression of M and E genes was performed as described in the legend to Fig. 2. The different M genes tested are indicated above the gels.

also sensitive to changes in the amino-terminal domain, i.e., the luminal domain of the M protein. For this purpose another set of mutants was constructed with various mutations in this domain. In mutant A_2A_3, the serines at positions 2 and 3 were replaced by alanines, while in mutant A_4A_5, the threonines at positions 4 and 5 were replaced by alanines (Fig. 1). Mutant ΔN lacks residues A_7 through F_{22}, resulting in an internal deletion of 16 amino acids. Three mutants have substitutions in this domain. In mutant A_8A_{10}, the prolines at positions 8 and 10 were replaced by alanines. $A_8A_{10}C_{14}$ also has a cysteine substitution for the tryptophan at position 14, which was fortuitously obtained during the construction of mutant A_8A_{10}. Mutant $G_{11}N_{13}$ has replacements of valine and glutamine at positions 11 and 13 with glycine and asparagine, respectively. Furthermore, two mutants with insertions between the initiating methionine and the serine at position 2 were constructed. Mutant Ains2 has an insertion of 1 alanine, while mutant His has a stretch of 6 histidines inserted for purification purposes. The mutant constructs were expressed alone and in combination with the E protein gene. Cells and media were processed and analyzed as described above. Analysis of the cell lysates (Fig. 5) demonstrated that in all cases mutant M proteins of expected sizes were expressed but that their glycosylation patterns were variously affected. It should be noted that O glycosylation of MHV M occurs at a threonine in the amino-terminal domain (unpublished data). Thus, mutant A_4A_5 did not become glycosylated, and this did not reflect an inability to be transported to the Golgi complex, as was verified by immunofluorescence (Fig. 3E). The same holds true for mutant ΔN; the deletion blocked glycosylation at the threonines without affecting intracellular transport (Fig. 3D). Transport was also unaffected for mutants A_8A_{10} and $A_8A_{10}C_{14}$ (Fig. 3F and G). The extents of glycosylation of these mutants were decreased, apparently due to the replacements of the prolines. The normal pattern of differently glycosylated species was observed with mutants A_2A_3, $G_{11}N_{13}$ and Ains2. The His mutant also showed the usual pattern of glycosylation, indicating that the insertion of the histidine stretch did not interfere with the membrane translocation of the amino-terminal domain, which occurs through the action of an internal signal sequence (61). The normal glycosylation also indicates that the protein's transport to the Golgi complex was not affected. One reason to prepare mutant $G_{11}N_{13}$ was to obtain an N-glycosylated form of MHV M. The N glycosylation consensus sequence generated by the introduction of the asparagine at position 13 appeared, however, not to be used by the cell. The protein's modifications are indistinguishable from those of WT M and are insensitive to endoglycosidases that remove N-linked sugars.

In considering VLP formation, it is clear from Fig. 5 that all mutant M proteins failed to be secreted into the culture medium when expressed alone. When coexpressed with the E protein, mutants A_2A_3 and A_4A_5 were secreted into the medium with efficiency similar to that of WT M. This result indicated that neither the serines nor the threonines are primary structure requirements for VLP formation. Interestingly, O glycosylation of the M protein is not a prerequisite for VLP assembly and release, since the unglycosylated mutant A_4A_5

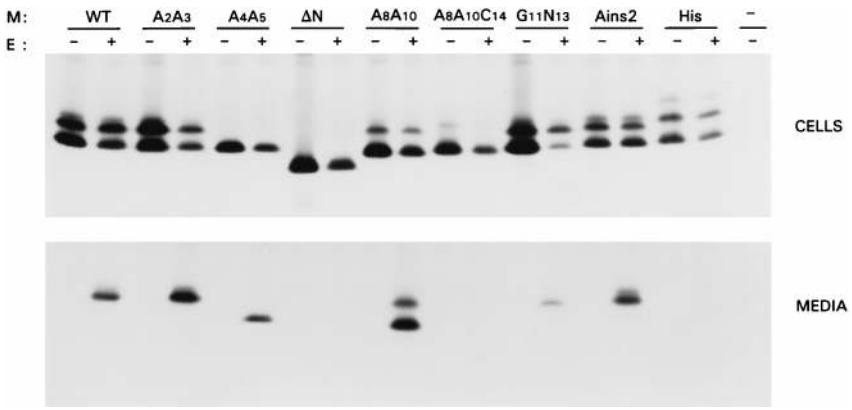

FIG. 5. Effects of mutations in the amino-terminal domain of M on VLP assembly. M and E genes were expressed as described in the legend to Fig. 2.

was found in the medium. Mutant ΔN was not secreted, indicating that the deleted part of the amino-terminal domain is important for VLP formation. Consistently, other mutations in this region also showed drastic effects: mutant $G_{11}N_{13}$ had reduced VLP-forming ability, while complete inhibition was observed with mutant $A_8A_{10}C_{14}$. Since mutant A_8A_{10} was secreted efficiently, the prolines do not seem to be important. The relatively high proportion of the unglycosylated form of the secreted protein reflects the decreased extent of glycosylation of this mutant. When mutant $A_8A_{10}C_{14}$ was analyzed under nonreducing conditions, it was resolved as a monomer (data not shown), indicating that the cysteine introduced at position 14 did not lead to formation of a disulfide bridge between M molecules. Mutant Ains2 was secreted into the medium efficiently; hence, it is clear that insertion of 1 alanine at position 2 does not affect the ability of the M protein to form VLPs. Insertion of the histidine stretch, however, strongly impaired VLP assembly, indicating that only minor insertions are allowed at this position.

Assembly of N-glycosylated M protein in VLPs. Coronavirus M proteins are either N glycosylated or O glycosylated in the amino-terminal domain (62). Murine coronaviruses belong to the latter category. Above we showed that O glycosylation is not required for MHV membrane assembly. In order to investigate whether MHV M would still be able to function in assembly as an N-glycosylated protein, we constructed a mutant (S_2N) in which the serine residue at position 2 was replaced by an asparagine, thus creating an N glycosylation consensus sequence (Asn-X-Ser/Thr [22]). The mutant construct was expressed alone or in combination with the E protein gene. Initial expression studies with the mutant showed that the protein can become both O and N glycosylated in a complex pattern that will be described elsewhere (unpublished data). One major complication was the maturation of the N-linked side chain by extensive heterogeneous modifications, resulting in a diffuse smear in the gel, which hampered the detection of N-glycosylated M protein in cells and VLPs. In order to avoid this problem, we used an inhibitor of oligosaccharide maturation, 1-deoxy-mannojirimycin (DMJ), which interferes with the action of α-mannosidase I, keeping the sugars in a simple, endoglycosidase H (endo H)-sensitive form (21). In other cases, cells were treated with tunicamycin, a general inhibitor of N glycosylation (reviewed by Elbein [14]). Cells and media were processed and analyzed as described above. Prior to gel electrophoresis, some immunoprecipitates were treated with glyco F to remove the N-linked sugars. Analysis of the cell lysates (Fig. 6) showed the mutant S_2N protein to appear both in an unglycosylated form (lower band; about 23 kDa) and as some N-glycosylated species (lanes 5 and 6). The distinct band of about 28 kDa consisted of M protein carrying N-linked sugars that were endo H sensitive (data not shown). The endo-H-resistant S_2N was differentially glycosylated and could not be distinguished from the background due to its heterogeneity. After treatment with glyco F, the N-linked sugars were removed, resulting in the typical pattern of differently O-glycosylated M species (Fig. 6, lanes 7 and 8). Hence, S_2N was both N and O glycosylated. After treatment with DMJ, the N-glycosylated M proteins appeared as a 28- and a 30-kDa species (Fig. 6, lanes 9 and 10). When immunoprecipitates were treated with glyco F, the typical pattern of differently O-glycosylated M species was again observed (Fig. 6, lanes 11 and 12). DMJ did not influence expression of WT M quantitatively or qualitatively (Fig. 6, lanes 3 and 4). Treatment of S_2N-expressing cells with tunicamycin resulted in S_2N that was O glycosylated but not N glycosylated (Fig. 6, lanes 13 and 14).

Analysis of the media (Fig. 6) showed that when the S_2N mutant was coexpressed with E in the absence of DMJ (lanes 5 to 8), little S_2N was detected in the medium. None of the unglycosylated form and hardly any of the 28-kDa N-glycosylated form appeared to be released. Only some heterogeneously glycosylated M protein was secreted (Fig. 6, lane 6), partly representing double-glycosylated material, as became apparent after glyco F treatment (lane 8). VLP release was much higher when oligosaccharide maturation was prevented by DMJ (Fig. 6, lanes 9 to 12). Significant amounts of the now immature, double-glycosylated form were secreted into the medium. Apparently, N glycosylation per se did not affect VLP assembly strongly. DMJ itself had a slight but distinct inhibitory effect on VLP formation or release, as was clear from the interference with production of WT-based particles (Fig. 6, lanes 2 and 4). When N glycosylation of S_2N was blocked by using tunicamycin, normal amounts of VLPs, containing the normal O-glycosylated forms of M, were produced (Fig. 6, lane 14). Apparently, the mutation itself did not interfere with VLP assembly.

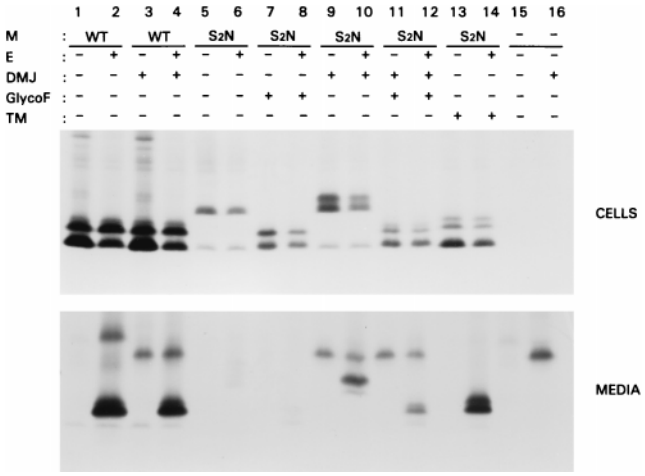

FIG. 6. Assembly of an N-glycosylated form of the MHV M protein into VLPs. OST7-1 cells infected with recombinant vaccinia virus vTF7-3 were transfected with a plasmid containing the WT or the S_2N mutant M gene, either alone or in combination with a plasmid containing the E protein gene, each gene behind a T7 promoter. Cells were labeled for 3 h with ^{35}S-labeled amino acids. In some cases, cells were treated with 1 mM DMJ (lanes 3 and 4, 9 to 12, and 16); in other cases, cells were treated with 5 μg of tunicamycin (TM)/ml (lanes 13 and 14). Both cells (upper panel) and the culture medium (lower panel) were prepared and used for immunoprecipitation, and the precipitates were analyzed by SDS-PAGE. Prior to gel electrophoresis, some immunoprecipitates were treated with glyco F to remove N-linked sugars (lanes 7, 8, 11, and 12).

Inhibition of normal VLP formation by M proteins with carboxy-terminal tail deletions. Interactions between M molecules are considered essential in coronavirus envelope assembly. It was therefore of interest to analyze whether and how mutant M proteins that are themselves deficient in VLP formation would interfere with the assembly of VLPs driven by WT M and E. Therefore, a triple-expression experiment in which these proteins were coexpressed with different carboxy-terminal tail mutants was performed. Fixed amounts of plasmid DNA encoding WT M and E were used in transfection, while an equal or a 5-times-lower amount of the plasmid DNAs specifying the mutant M proteins was used. Cells and media were processed as described above. Analysis of the cell lysates (Fig. 7) in all cases showed the differently glycosylated M species. Due to the small differences in size, mutants Δ5, Δ2, and Δ1 could not be discriminated from WT M. The unglycosylated form of mutant Δ18 could be distinguished, but its

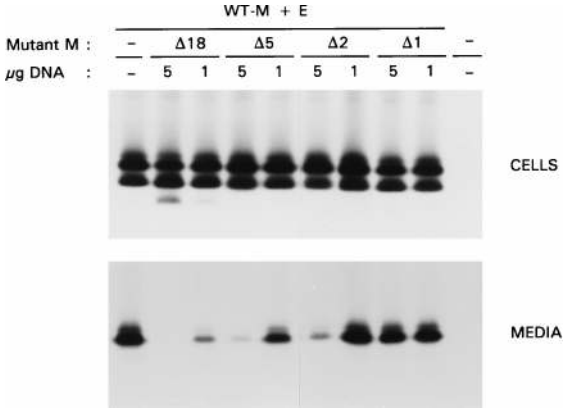

FIG. 7. Inhibition of VLP formation by mutant M proteins with carboxy-terminal deletions. After infection of OST7-1 cells with recombinant vaccinia virus vTF7-3, cells were transfected with plasmid DNA encoding WT M and E (5 μg of each) together with 1 or 5 μg of plasmid DNA encoding mutant M. The different M mutants expressed are indicated above the gels. Cells were labeled for 3 h with ^{35}S-labeled amino acids. Both cells (upper panel) and the culture medium (lower panel) were prepared and used for immunoprecipitation, and the precipitates were analyzed by SDS-PAGE.

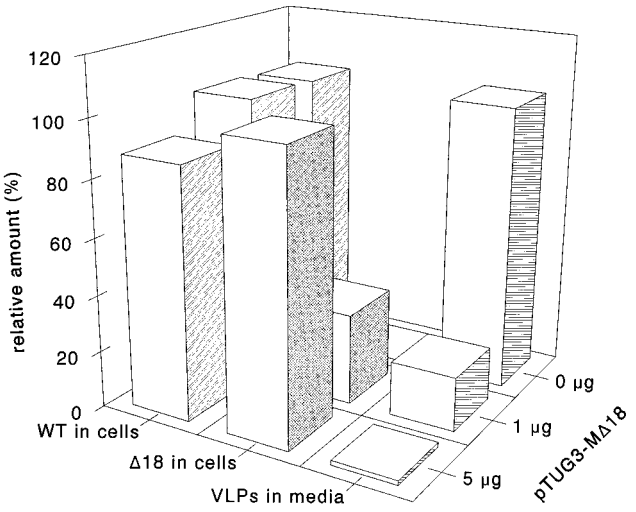

FIG. 8. Quantitation of the concentration-dependent inhibition of VLP formation by mutant M protein Δ18. The relative amounts of glycosylated WT or unglycosylated Δ18 mutant M protein present in cells and media for each transfection condition shown in Fig. 6 were determined by using a phosphorimager. The relative amount of WT M secreted (i.e., VLPs in media) is also shown.

glycosylated forms were also obscured by WT M. In this case the glycosylated species of WT M could be discriminated from those of the mutant because the former run slightly slower. The results indicate that the expression of WT M was hardly affected by the coexpression of mutant Δ18, even when equal amounts of their plasmids had been cotransfected. Judging from the amounts of the unglycosylated forms, it seems that the efficiency of expression was higher for WT M than for the mutant.

Analysis of the media showed that the mutant M proteins inhibited VLP assembly in a concentration-dependent manner and that the extent of inhibition increased with an increasing extent of deletion. This is best illustrated by mutant Δ18. At the higher concentration, this protein caused an almost complete block of VLP formation. When its synthesis in cells was reduced to levels that were hardly detectable, VLP production became evident again, but the efficiency was severely decreased. Quantitation showed that VLP assembly increased 12 times when the concentration of Δ18 was about 3 times lower (Fig. 8). No mutant Δ18 protein could be detected in the medium. Similar observations were made with the mutants Δ5 and Δ2, but the effects became progressively weaker as the deletion was made smaller. Finally, the lack of just 1 terminal residue, as in mutant Δ1, did not show any measurable inhibitory effects on VLP formation.

Rescue of deletion mutants into VLPs. Our inability to discriminate between the WT M protein and the mutant M proteins in these competition experiments did not allow an accurate analysis of the possible rescue of the mutant proteins into VLPs. To circumvent this problem and to increase the sensitivity of detection, we made use of mutant A_2A_3, which we showed above to function efficiently in VLP assembly (Fig. 5). Moreover, we found that the mutations in this M protein destroyed the epitope recognized by the monoclonal antibody J1.3 (17). Replacing WT M by this mutant therefore allowed the desired discrimination. Rescue experiments were performed as described above. To allow sufficient VLP production, a 5-times-lower amount of plasmid DNA specifying the M proteins to be rescued was used compared to the amount of A_2A_3 plasmid. Analysis of the cell lysates (Fig. 9) showed that A_2A_3 protein is precipitated with the polyclonal anti-MHV serum k134 but not with the monoclonal antibody J1.3. When mutants Δ18, Δ5, Δ2, or Δ1 or WT M was coexpressed with mutant A_2A_3, M proteins were immunoprecipitated with the polyclonal anti-MHV serum. Only after prolonged exposure could M protein be detected in the samples immunoprecipitated with J1.3, indicating that under the conditions used, the bulk of the expressed M protein is A_2A_3.

Analysis of the media using the polyclonal anti-MHV serum showed that all combinations were productive in VLP formation. Mutant A_2A_3 was easily detected in the medium with the polyclonal serum but not with J1.3 antibodies. Immunoprecipitations with J1.3 showed that mutant M proteins, which were themselves deficient in VLP formation, could be rescued into particles by assembly-competent M. Under the experimental conditions used, A_2A_3 protein in the media was clearly coim-

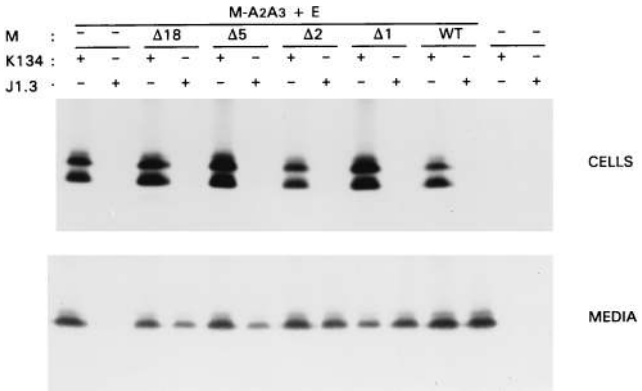

FIG. 9. Rescue of carboxy-terminal deletion mutant M proteins into VLPs. After infection of OST7-1 cells with recombinant vaccinia virus vTF7-3, cells were transfected with plasmid DNA encoding mutant M protein A_2A_3 and E protein (5 μg of each). In some cases, these were cotransfected with 1 μg of plasmid DNA encoding the indicated mutant or WT M protein. Cells were labeled for 3 h with ^{35}S-labeled amino acids. Both cells (upper panel) and the culture medium (lower panel) were prepared and used for immunoprecipitation, either with the polyclonal anti-MHV serum k134 or with the monoclonal antibody J1.3, and the precipitates were analyzed by SDS-PAGE.

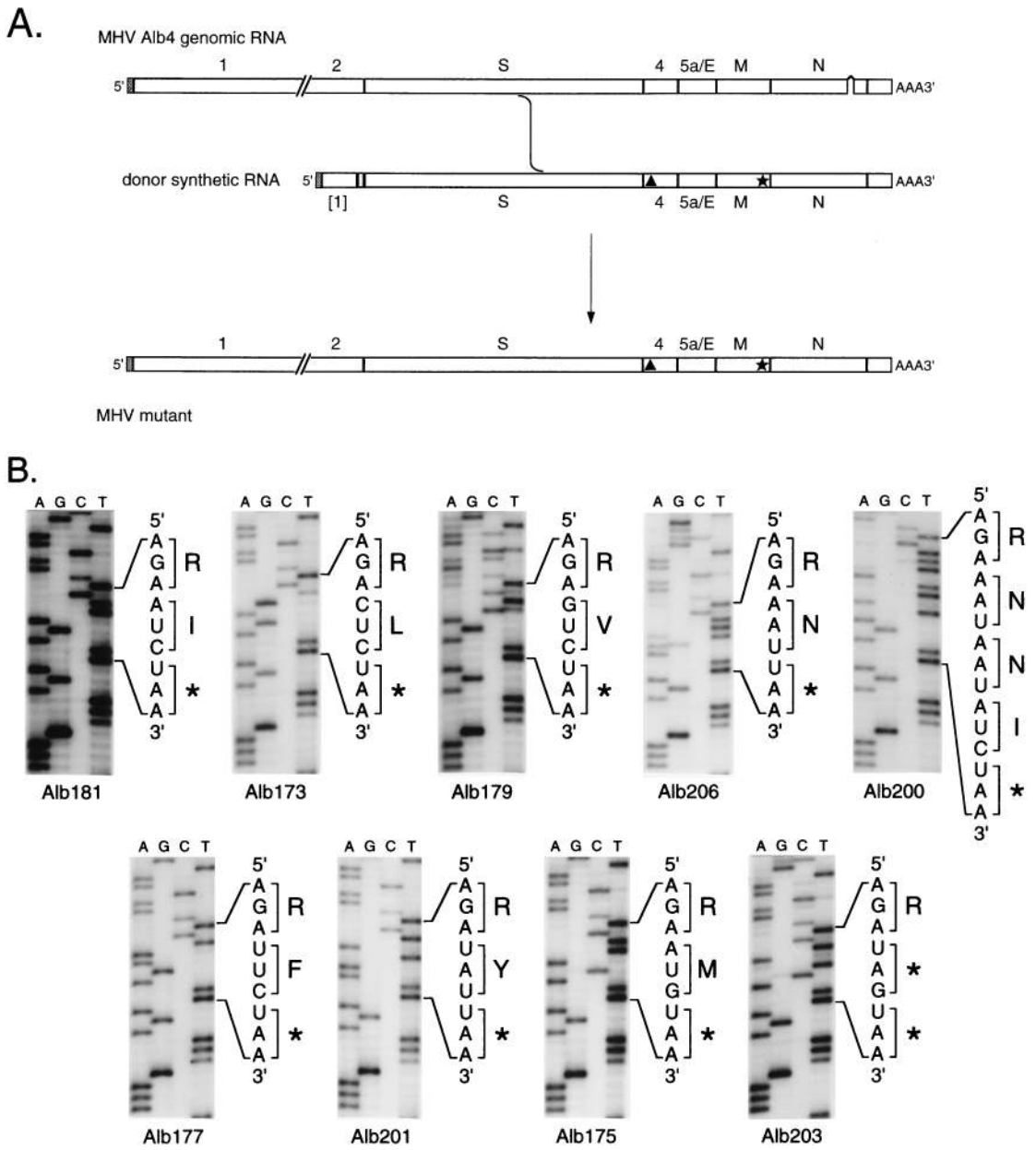

FIG. 10. Incorporation of M protein cytoplasmic-domain mutations into the MHV genome. (A) Schematic for construction of M mutants by targeted recombination between donor synthetic RNA and the N-gene deletion mutant Alb4. Each donor RNA containing a codon 228 mutation in the M gene (denoted by a star) was transcribed from a vector derived from pCFS8 (16), which includes the entire portion of the MHV genome 3′ to the start of the S gene and is tagged with a 19-base marker in gene 4 (denoted by a triangle). In the case shown, the MHV mutant, generated by a single upstream crossover, has inherited the gene 4 tag, the constructed M mutation, and the region repairing the N-gene deletion. (B) Sequence of the relevant region of genomic RNA isolated from passage-3 purified virions of one mutant of each type. For each codon 228 mutation, recombinants were obtained that contained and that lacked the upstream gene 4 tag. The particular mutants shown are all positive for the gene 4 tag, except for Alb206 and Alb200. For Alb200, a BCV-MHV chimeric M protein mutant, the donor RNA was derived from pFV1 (16) and did not contain the gene 4 tag.

munoprecipitated with the deletion mutant proteins, although these proteins themselves were synthesized at relatively low levels. Coimmunoprecipitation of A_2A_3 was interpreted as a measure for rescue of assembly-incompetent M proteins. It was more pronounced when the truncation was smaller, but even mutant Δ18 could still be rescued. These observations provide evidence for the existence of intermolecular interactions between M proteins in the viral particles.

Incorporation of cytoplasmic domain mutations into virions. To further our understanding of the consequences of M protein carboxy-terminal tail mutations in the presence of the full complement of virion structural components, we sought to directly introduce many of these mutations into the genome of MHV A59. This was accomplished by targeted RNA recombination between a synthetic defective interfering (DI) RNA analog containing one of the intended mutations and the N-gene deletion mutant Alb4 as the recipient virus (16, 45, 59) (Fig. 10A). In this manner we were able to isolate several recombinant viruses containing each of the carboxy-terminal residue substitutions that had been studied in the VLP system: $T_{228}I$, $T_{228}L$, $T_{228}V$, and $T_{228}N$ (Fig. 10B). Another recombinant was constructed in which the carboxy-terminal half of the

MHV M protein (amino acid residues 134 to 228) was replaced with its counterpart from BCV (residues 133 to 230), a region containing 17 amino acid differences from MHV, including the residues $NNI_{228-230}$ in place of T_{228} (Fig. 10B). In addition, the substitution mutants $T_{228}F$, $T_{228}Y$, and $T_{228}M$ were also created in the viral M protein (Fig. 10B). (The $T_{228}F$ mutant also contained a secondary mutation, $T_{228}I$.) With one exception, all of these M protein mutants had plaque sizes indistinguishable from that of the WT virus, and at passage 3 all had high yields in tissue culture ($>10^8$ PFU/ml), comparable to or better than that of the WT. For a subset of the mutants, $T_{228}I$, $T_{228}V$, and $T_{228}N$, virus stocks were serially propagated for six passages. Following every passage the genetic stability of each mutant was monitored by direct sequencing of an RT-PCR product of the region containing the constructed mutation. None of the sequences showed any detectable reversion or other secondary genetic alteration, indicating that the introduced genomic changes were stable for at least six passages. The only phenotypic difference noted was with $T_{228}V$ mutants, which, for both of the independent recombinants analyzed, exhibited a slightly smaller plaque size than the WT at 39°C. These results showed that assembly of the complete virion of MHV tolerates changes in the carboxy-terminal residue of the M protein that are considerably more deleterious for the formation of particles from just the M and E proteins (Fig. 4). In the most extreme case, the $T_{228}N$ mutation, which severely diminished VLP production, had no obvious phenotypic effect when incorporated into MHV. As can be seen in Fig. 10B, direct sequencing of RNA isolated from highly purified virions of the $T_{228}N$ mutant Alb206 revealed a substantial amount of overlapping sequence from the leader region of subgenomic RNA 7, which was read by the same primer. This was observed in multiple independent preparations of purified virions of this mutant and of an independent $T_{228}N$ mutant, Alb205. For Alb205, we confirmed the presence of the mutant asparagine codon by sequencing an RT-PCR product from the M-N junction region of the viral genome. We have previously noted that highly purified MHV contains a small amount of packaged subgenomic RNAs (60). It remains for further work to determine if the $T_{228}N$ mutants aberrantly package greater amounts of these RNA species.

We next attempted to introduce the Δ1, Δ2, Δ5, and Δ18 mutations into MHV to investigate their effects on the stability and assembly of virions. These mutants were designed by replacing the respective residues from the carboxy terminus of M with one stop codon (for Δ1 and Δ2) or two stop codons in tandem (for Δ5 and Δ18). This approach was taken in order to avoid unintended effects on the transcription of the downstream N gene that might have resulted from the actual deletion of RNA sequences at the 3′ terminus of the M gene adjacent to the M-N intergenic sequence. Somewhat surprisingly, we were able to isolate recombinants containing the Δ1 mutation (Fig. 10B), which had been lethal for VLP assembly (Fig. 2). This mutant was not only viable but was phenotypically indistinguishable from the WT in plaque size and in viral yield, and it exhibited no detectable accumulation of revertants after six passages. This again points to the existence of interactions in the complete assembled virion that must promote further stability beyond that obtained in VLPs composed solely of M and E proteins.

By contrast, in multiple targeted recombination experiments, we were not able to construct recombinants harboring either the Δ2, Δ5, or Δ18 mutation. In each case, recombinant candidates obtained with these donor synthetic RNAs were analyzed for the acquisition of three markers: (i) repair of the Alb4 N-gene deletion, (ii) the M-gene mutation, and (iii) a phenotypically silent 19-base tag in gene 4 (16) (Fig. 10A). Of 24 recombinants arising from four independent experiments with the Δ2 mutant donor RNA, all of which had repaired the N-gene deletion, none contained either the Δ2 mutation or the gene 4 tag. This suggests, but does not prove, that the Δ2 mutation is lethal to the virus. It is currently unclear why we have not yet obtained gene 4-tagged recombinants from the Δ2 mutant donor RNA. Experiments now underway are aimed at the possibility of recovering the Δ2 mutant if it has a conditional lethal phenotype. Of 12 recombinant viruses obtained from four independent experiments with the Δ5 mutant donor RNA, all had repaired the N-gene deletion but none contained the Δ5 mutation. Most notably, 7 of the 12 also had the gene 4 tag, indicating that each of these must have been derived from at least three crossover events between the donor RNA and the recipient Alb4 genome (Fig. 10A). Similarly, 12 recombinants representing four independent sets from the Δ18 mutant donor RNA did not contain the Δ18 mutation, although all had repaired the N-gene deletion, and 5 of the 12 also had the gene 4 tag. This presence of inherited markers both upstream and downstream of the excluded M-gene mutations provides compelling evidence that the Δ5 and Δ18 mutations are lethal to the virus. Thus, in agreement with the results generated in the VLP system, the carboxy terminus of the M protein must also play a critical role in assembly of the whole virion.

DISCUSSION

Despite a high degree of sequence variation among the coronavirus M proteins, there is a surprising conservation of their overall chemical features (reviewed by Rottier [62]). The dominant common feature is the occurrence of three hydrophobic domains alternating with short hydrophilic regions. The carboxy-terminal half of all M proteins is largely amphiphilic, with a hydrophilic end. This conservation indicates that there are rigid structural constraints on M as a result of functional requirements. Indeed, M has been shown to play a key role in coronavirus assembly. M and E are the only requirements for particle formation (73). Using an envelope assembly assay, we have now shown that all domains of the M protein are important. Changes in the primary structure of the luminal domain, the transmembrane cluster, the amphiphilic domain, and the carboxy-terminal domain had effects on the assembly of M into enveloped particles. Clearly, in order for M to function in assembly, stringent requirements must be satisfied.

The carboxy-terminal domain is located in the cytoplasm. In infected cells this domain is probably important for virus assembly by interacting with the nucleocapsid. An affinity of M for nucleocapsids has been observed in vitro with several coronaviruses. Subviral particles prepared by NP-40 disruption of purified MHV (70, 75), avian IBV (39), or BCV (32) still contained M protein associated with the nucleocapsids. Our results indicate that this cytoplasmic domain is also of crucial importance for the assembly of the viral envelope. Both the exposed carboxy end and the amphiphilic, protease-resistant domain between this end and the transmembrane domains appeared to be essential structural requirements. Strikingly, the extreme carboxy-terminal residues were found to be crucial. The VLP system provided the most sensitive indicator of this: deletion of as little as the single terminal residue of M protein (Δ1) was fatal, while substitutions or extensions at this position generally had a strong negative effect on assembly. Relative to this, in the whole virus the threshold for loss of function was slightly displaced. The Δ1 mutation had no detectable effect when incorporated into the MHV genome, and

only one of eight different substitutions of the carboxy-terminal residue had a weakly measurable impact on viral phenotype. These results suggest that in the complete virion an additional component, most likely the nucleocapsid, provides a further measure of stabilization not available in VLPs composed purely of M and E proteins. Moreover, there may be other factors, such as the kinetics of virion assembly or the relative or absolute levels of viral protein expression, that render the whole virus more tolerant to mutational changes that are devastating in the VLP system. Nevertheless, further truncation of the M protein carboxy terminus in the virion, as in the VLP system, appeared to abrogate its function. In multiple attempts, we were unable to incorporate the Δ2, Δ5, or Δ18 mutation into the MHV genome, suggesting that these mutations, if not absolutely lethal, were at least as harmful to the virus as the lesion in Alb4, the N deletion mutant from which recombinants were selected. These observations all point to a sensitive role of the extreme terminal residues in some aspect of envelope assembly. The exact nature of this role remains unclear, but it is not unlikely that the very carboxy terminus is involved in interactions either intramolecularly, to establish a particular secondary structure in the M molecule, or intermolecularly, with membrane lipids, with E, or with other M proteins. A role of the carboxy terminus in homotypic interactions is, however, unlikely in view of earlier data. Using sucrose gradient analysis, we have shown previously that the MHV M protein alone can associate into large homomeric complexes (36), but this oligomerization still occurred when the carboxy-terminal 22 residues of the protein were deleted.

The cytoplasmic domain of envelope proteins has been assigned an important role in the assembly of many enveloped viruses. It was shown to be essential for incorporation of the glycoprotein of vesicular stomatitis virus (57, 76). For alphaviruses the cytoplasmic domain of the E2 envelope glycoprotein appeared to be critical, with particular roles for a tyrosine, a leucine, and a set of cysteines important for palmitoylation (29, 56, 78). Interestingly, the 2-residue cytoplasmic tail of glycoprotein E1 is dispensable for virus growth (4). In the case of retroviruses, a direct interaction in vitro was reported between the matrix protein and the cytoplasmic domain of the Env protein of human immunodeficiency virus type 1 (HIV-1) (8). Deletions in the cytoplasmic domain of the Env protein of HIV-1 (11, 18, 77) and murine leukemia virus (24) affect Env incorporation into virions. Remarkably, HIV-1 Env mutants with large cytoplasmic deletions can be incorporated into virions in a matrix-independent manner (19, 43). The influenza virus hemagglutinin (HA) cytoplasmic tail is not essential for virus assembly (30, 52, 68). However, deletion of the cytoplasmic tail of influenza virus neuraminidase (NA) severely compromised the incorporation of mutant NA molecules into virions (5, 49).

The amino-terminal domain of the coronaviral M protein is exposed luminally in cellular organelles. This domain varies considerably in length, from some 16 residues in the mature protein of the human coronavirus (HCV) 229E to around 36 in that of feline coronaviruses (see reference 62). No function has been assigned to it yet. Somewhat to our surprise, some changes in this domain did affect MHV VLP formation. At the very amino terminus, insertion of a single residue (alanine) following the initiating methionine was allowed, but a six-His stretch at this position was nearly fatal. Changes in the clusters of hydroxyl amino acids flanking the methionine, or substitutions of the two nearby prolines, were without effect. In contrast, deletion of the middle part of the ectodomain or some substitutions in this domain had severe effects. One such substitution involved a fortuitously obtained tryptophan-to-cysteine mutation at a position close to that where a cysteine naturally occurs in the HCV 229E M protein. While the latter cysteine gives rise to the formation of homodimers (3), no disulfide bonds were observed with the MHV M mutant protein. For alphaviruses, mutations in the ectodomain of the envelope proteins have been shown to affect virus assembly (12, 25, 41). It was suggested that these mutations resulted in impaired lateral interactions causing the budding defect. This might also be the explanation for the behavior of the amino-terminal M mutants.

Coronavirus M proteins are invariably glycosylated, carrying either N-linked or O-linked oligosaccharides (see reference 62). The oligosaccharides are attached to the amino-terminal region of the M molecule and are thus exposed at the virion surface. Since a function for this modification has not been identified, we used our VLP system to study the possible involvement of glycosylation in virus assembly. Our results showed that for MHV, O glycosylation of the M protein is not required. We then created an N-glycosylated form of the protein which appeared still to produce particles, though with decreased efficiency. Only when the maturation of the N-linked oligosaccharide was inhibited did VLP production become normal, indicating that N glycosylation per se was not interfering with assembly. Altogether, these observations demonstrate that glycosylation plays no role in assembly, consistent with the findings of earlier studies that used tunicamycin (69) and monensin (53) to inhibit glycosylation in infected cells. In addition, Laude et al. (40) isolated a mutant of the porcine TGEV in which the sole N-glycosylation site of the M protein had been disrupted without affecting the viability of the virus.

As mentioned above, homotypic interactions between M molecules are supposed to be essential in coronavirus envelope formation. It was therefore of interest to investigate whether M molecules that are themselves deficient in VLP formation would interfere with the formation of particles by assembly-competent M and E. From the set of carboxy-terminal tail deletion mutants of M that we studied, it was clear that interference indeed occurred, in a concentration-dependent manner. Furthermore, assembly-competent M protein was able to rescue assembly-negative M molecules into particles. These observations support the importance of lateral interactions between M molecules in the assembly process. Moreover, they also support our earlier conclusion that such interactions do not require the cytoplasmic tail of the M protein. This conclusion was based on the finding that a mutant M protein lacking the carboxy-terminal 22 amino acids was able to associate into large heterogeneous complexes as does WT M, as shown by sucrose density gradient analysis (36). Lateral interactions between envelope proteins have similarly been demonstrated for Semliki Forest virus. Here it was shown that nucleocapsid binding-deficient p62-E1 heterodimers did inhibit normal virus budding in a concentration-dependent way and that under suitable conditions these heterodimers could be rescued into virus particles (13). It is quite likely that lateral interactions between viral glycoproteins generally are instrumental in the assembly of enveloped viruses.

ACKNOWLEDGMENTS

We are grateful to Peggy Roestenberg, Marèl de Wit, and Chantal Vogelzangs for their assistance in part of the experimental work. We thank David Brian (University of Tennessee) for generously providing the clone p(M+N)CAT1.

These investigations were supported by financial aid from the Netherlands Foundation for Chemical Research (SON) and the Netherlands Organization for Scientific Research (NWO) to C.A.M. de H. and by grant AI 39544 from the National Institutes of Health to P.S.M.

REFERENCES

1. **Allison, S. L., K. Stadler, C. W. Mandl, C. Kunz, and F. X. Heinz.** 1995. Synthesis and secretion of recombinant tick-borne encephalitis virus protein E in soluble and particulate form. J. Virol. **69:**5816–5820.
2. **Armstrong, J., H. Niemann, S. Smeekens, P. Rottier, and G. Warren.** 1984. Sequence and topology of a model intracellular membrane protein, E1 glycoprotein, from a coronavirus. Nature **308:**751–752.
3. **Arpin, N., and P. J. Talbot.** 1990. Molecular characterization of the 229E strain of human coronavirus. Adv. Exp. Med. Biol. **276:**73–80.
4. **Barth, B. U., M. Suomalainen, P. Liljeström, and H. Garoff.** 1992. Alphavirus assembly and entry: role of the cytoplasmic tail of the E1 spike subunit. J. Virol. **66:**7560–7564.
5. **Bilsel, P., M. R. Castrucci, and Y. Kawaoka.** 1993. Mutations in the cytoplasmic tail of influenza A virus neuraminidase affect incorporation into virions. J. Virol. **67:**6762–6767.
6. **Bos, E. C., W. Luytjes, H. V. van der Meulen, H. K. Koerten, and W. J. M. Spaan.** 1996. The production of recombinant infectious DI-particles of a murine coronavirus in the absence of helper virus. Virology **218:**52–60.
7. **Brian, D. A., B. G. Hogue, and T. E. Kienzle.** 1995. The coronavirus hemagglutinin esterase glycoprotein, p. 165–179. *In* S. G. Siddell (ed.), The Coronaviridae. Plenum Press, New York, N.Y.
8. **Cosson, P.** 1996. Direct interaction between the envelope and matrix protein of HIV-1. EMBO J. **15:**5783–5788.
9. **Delchambre, M., D. Gheysen, D. Thines, C. Thiriart, E. Jacobs, E. Verdin, M. Horth, A. Burny, and F. Bex.** 1989. The Gag precursor of simian immunodeficiency virus assembles into virus-like particles. EMBO J. **8:**2653–2660.
10. **de Vries, A. A. F., M. J. B. Raamsman, H. A. van Dijk, M. C. Horzinek, and P. J. M. Rottier.** 1995. The small envelope glycoprotein (G_S) of equine arteritis virus folds into three distinct monomers and a disulfide-linked dimer. J. Virol. **69:**3441–3448.
11. **Dubay, J. W., S. J. Roberts, B. H. Hahn, and E. Hunter.** 1992. Truncation of the human immunodeficiency virus type 1 transmembrane glycoprotein cytoplasmic domain blocks virus infectivity. J. Virol. **66:**6616–6625.
12. **Duffus, W. A., P. Levy-Mintz, M. R. Klimjack, and M. Kielian.** 1995. Mutations in the putative fusion peptide of Semliki Forest virus affect spike protein oligomerization and virus assembly. J. Virol. **69:**2471–2479.
13. **Ekström, M., P. Liljeström, and H. Garoff.** 1994. Membrane protein lateral interactions control Semliki Forest virus budding. EMBO J. **13:**1058–1064.
14. **Elbein, D. A.** 1987. Inhibitors of the biosynthesis and processing of N-linked oligosaccharide chains. Annu. Rev. Biochem. **56:**497–534.
15. **Elroy-Stein, O., and B. Moss.** 1990. Cytoplasmic expression system based on constitutive synthesis of bacteriophage T7 RNA polymerase in mammalian cells. Proc. Natl. Acad. Sci. USA **87:**6743–6747.
16. **Fischer, F., C. F. Stegen, C. A. Koetzner, and P. S. Masters.** 1997. Analysis of a recombinant mouse hepatitis virus expressing a foreign gene reveals a novel aspect of coronavirus transcription. J. Virol. **71:**5148–5160.
17. **Fleming, J. O., R. A. Shubin, M. A. Sussman, N. Casteel, and S. A. Stohlman.** 1989. Monoclonal antibodies to the matrix (E1) glycoprotein of mouse hepatitis virus protect mice from encephalitis. Virology **168:**162–167.
18. **Freed, E. O., and M. A. Martin.** 1996. Domains of the human immunodeficiency virus type 1 matrix and gp41 cytoplasmic tail required for envelope incorporation into virions. J. Virol. **70:**341–351.
19. **Freed, E. O., and M. A. Martin.** 1995. Virion incorporation of envelope glycoproteins with long but not short cytoplasmic tails is blocked by specific, single amino acid substitutions in the human immunodeficiency virus type 1 matrix. J. Virol. **69:**1984–1989.
20. **Fuerst, T. R., E. G. Niles, F. W. Studier, and B. Moss.** 1986. Eukaryotic transient-expression system based on recombinant vaccinia virus that synthesizes bacteriophage T7 RNA polymerase. Proc. Natl. Acad. Sci. USA **83:**8122–8126.
21. **Fuhrmann, U., E. Bause, G. Legler, and H. Ploegh.** 1984. Novel mannosidase inhibitor blocking conversion of high mannose to complex oligosaccharides. Nature **307:**755–758.
22. **Gavel, Y., and G. von Heijne.** 1990. Sequence differences between glycosylated and non-glycosylated Asn-X-Thr/Ser acceptor sites: implications for protein engineering. Protein Eng. **3:**433–442.
23. **Gheysen, D., E. Jacobs, A. de Foresta, C. Thiriart, M. Francotte, D. Thines, and M. De Wilde.** 1989. Assembly and release of HIV-1 precursor Pr55gag virus-like particles from recombinant baculovirus-infected cells. Cell **59:**103–112.
24. **Gray, K. D., and M. J. Roth.** 1993. Mutational analysis of the envelope gene of Moloney murine leukemia virus. J. Virol. **67:**3489–3496.
25. **Hahn, C. S., C. M. Rice, E. G. Strauss, E. M. Lenches, and J. H. Strauss.** 1989. Sindbis virus *ts*103 has a mutation in glycoprotein E2 that leads to defective assembly of virions. J. Virol. **63:**3459–3465.
26. **Hobman, T. C., M. L. Lundstrom, C. A. Mauracher, L. Woodward, S. Gilliam, and M. G. Farquhar.** 1994. Assembly of rubella virus structural proteins into virus-like particles in transfected cells. Virology **202:**574–585.
27. **Holmes, K. V., E. W. Doller, and L. S. Sturman.** 1981. Tunicamycin resistant glycosylation of coronavirus glycoprotein: demonstration of a novel type of viral glycoprotein. Virology **115:**334–344.
28. **Homberger, F. R.** 1994. Nucleotide sequence comparison of the membrane protein genes of three enterotropic strains of mouse hepatitis virus. Virus Res. **31:**49–56.
29. **Ivanova, L., and M. J. Schlesinger.** 1993. Site-directed mutations in the Sindbis virus E2 glycoprotein identify palmitoylation sites and affect virus budding. J. Virol. **67:**2546–2551.
30. **Jin, H., G. P. Leser, and R. A. Lamb.** 1994. The influenza virus hemagglutinin cytoplasmic tail is not essential for virus assembly or infectivity. EMBO J. **13:**5504–5515.
31. **Karacostas, V., K. Nagashima, M. A. Gonda, and B. Moss.** 1989. Human immunodeficiency virus-like particles produced by a vaccinia virus expression vector. Proc. Natl. Acad. Sci. USA **86:**8964–8967.
32. **King, B., and D. A. Brian.** 1982. Bovine coronavirus structural proteins. J. Virol. **42:**700–707.
33. **Klumperman, J., J. Krijnse Locker, A. Meijer, M. C. Horzinek, H. J. Geuze, and P. J. M. Rottier.** 1994. Coronavirus M proteins accumulate in the Golgi complex beyond the site of virion budding. J. Virol. **68:**6523–6534.
34. **Krijnse Locker, J., G. Griffiths, M. C. Horzinek, and P. J. M. Rottier.** 1992. O-glycosylation of the coronavirus M protein. Differential localization of sialyltransferases in N- and O-glycosylation. J. Biol. Chem. **267:**14094–14101.
35. **Krijnse Locker, J., M. Ericsson, P. J. M. Rottier, and G. Griffiths.** 1994. Characterization of the budding compartment of mouse hepatitis virus: evidence that transport from the RER to the Golgi complex requires only one vesicular transport step. J. Cell Biol. **124:**55–70.
36. **Krijnse Locker, J., D.-J. E. Opstelten, M. Ericsson, M. C. Horzinek, and P. J. M. Rottier.** 1995. Oligomerization of a trans-Golgi/trans-Golgi network retained protein occurs in the Golgi complex and may be part of its retention. J. Biol. Chem. **270:**8815–8821.
37. **Krijnse Locker, J., J. K. Rose, M. C. Horzinek, and P. J. M. Rottier.** 1992. Membrane assembly of the triple-spanning coronavirus M protein; individual transmembrane domains show preferred orientation. J. Biol. Chem. **267:**21911–21918.
38. **Laemmli, U. K.** 1970. Cleavage of structural proteins during assembly of the head of bacteriophage T4. Nature **227:**680–685.
39. **Lanser, J. A., and C. R. Howard.** 1980. The polypeptides of infectious bronchitis virus (IBV-41 strain). J. Gen. Virol. **46:**349–361.
40. **Laude, H., J. Gelfi, L. Lavenant, and B. Charley.** 1992. Single amino acid changes in the viral glycoprotein M affect induction of alpha interferon by the coronavirus transmissible gastroenteritis virus. J. Virol. **66:**743–749.
41. **Lindqvist, B. H., J. DiSalvo, C. M. Rice, J. H. Strauss, and E. G. Strauss.** 1986. Sindbis virus mutant ts20 of complementation group E contains a lesion in glycoprotein E2. Virology **151:**10–20.
42. **Lopez, S., J.-S. Yao, R. J. Kuhn, E. G. Strauss, and J. H. Strauss.** 1994. Nucleocapsid-glycoprotein interactions required for assembly of alphaviruses. J. Virol. **68:**1316–1323.
43. **Mammano, F., E. Kondo, J. Sodroski, A. Bukovsky, and H. G. Göttlinger.** 1995. Rescue of human immunodeficiency virus type 1 matrix protein mutants by envelope glycoproteins with short cytoplasmic domains. J. Virol. **69:**3824–3830.
44. **Mason, P. W., S. Pincus, M. J. Fournier, T. L. Mason, R. E. Shope, and E. Paoletti.** 1991. Japanese encephalitis virus-vaccinia recombinants produce particulate forms of the structural membrane proteins and induce high levels of protection against lethal JEV infection. Virology **180:**294–305.
45. **Masters, P. S., C. A. Koetzner, C. A. Kerr, and Y. Heo.** 1994. Optimization of targeted RNA recombination and mapping of a novel nucleocapsid gene mutation in the coronavirus mouse hepatitis virus. J. Virol. **68:**328–337.
46. **Mayer, T., T. Tamura, M. Falk, and H. Niemann.** 1988. Membrane integration and intracellular transport of the coronavirus glycoprotein E1, a class III membrane glycoprotein. J. Biol. Chem. **263:**14956–14963.
47. **Mead, D. A., E. Szczesna-Skorupa, and B. Kemper.** 1986. Single-stranded DNA 'blue' T7 promoter plasmids: a versatile tandem promoter system for cloning and protein engineering. Protein Eng. **1:**67–74.
48. **Mebatsion, T., M. König, and K.-K. Conzelman.** 1996. Budding of rabies virus particles in the absence of the spike glycoprotein. Cell **84:**941–951.
49. **Mitnaul, L. J., M. R. Castrucci, K. G. Murti, and Y. Kawaoka.** 1996. The cytoplasmic tail of influenza A virus neuraminidase (NA) affects NA incorporation into virions, virion morphology, and virulence in mice but is not essential for virus replication. J. Virol. **70:**873–879.
50. **Moremen, K. W., O. Touster, and P. W. Robbins.** 1991. Novel purification of the catalytic domain of a Golgi α-mannosidase II: characterization and comparison with the intact enzyme. J. Biol. Chem. **266:**16876–16885.
51. **Mounir, S., and P. J. Talbot.** 1992. Sequence analysis of the membrane protein gene of human coronavirus OC43 and evidence for O-glycosylation. J. Gen. Virol. **73:**2731–2736.
52. **Naim, H. Y., and M. G. Roth.** 1993. Basis for selective incorporation of glycoproteins into the influenza virus envelope. J. Virol. **67:**4831–4841.
53. **Niemann, H., B. Boschek, D. Evans, M. Rosing, T. Tamura, and H. D. Klenk.** 1982. Post-translational glycosylation of coronavirus glycoprotein E1: inhibition by monensin. EMBO J. **1:**1499–1504.
54. **Niemann, H., G. Heisterberg-Moutsis, R. Geyer, H.-D. Klenk, and M. Wirth.** 1984. Glycoprotein E1 of MHV-A59: structure of the O-linked carbohydrates and construction of full length cDNA clones. Adv. Exp. Med. Biol. **173:**201–213.

55. **Opstelten, D. J., M. J. Raamsman, K. Wolfs, M. C. Horzinek, and P. J. M. Rottier.** 1995. Envelope glycoprotein interactions in coronavirus assembly. J. Cell Biol. **131:**339–349.
56. **Owen, K. E., and R. J. Kuhn.** 1997. Alphavirus budding is dependent on the interaction between the nucleocapsid and hydrophobic amino acids on the cytoplasmic domain of the E2 envelope glycoprotein. Virology **230:**187–196.
57. **Owens, R. J., and J. K. Rose.** 1993. Cytoplasmic domain requirement for incorporation of a foreign envelope protein into vesicular stomatitis virus. J. Virol. **67:**360–365.
58. **Patzer, E. J., G. R. Nakamura, C. C. Simonsen, A. D. Levinson, and R. Brands.** 1986. Intracellular assembly and packaging of hepatitis B surface antigen particles occur in the endoplasmic reticulum. J. Virol. **58:**884–892.
59. **Peng, D., C. A. Koetzner, T. McMahon, Y. Zhu, and P. S. Masters.** 1995. Construction of murine coronavirus mutants containing interspecies chimeric nucleocapsid proteins. J. Virol. **69:**5475–5484.
60. **Peng, D., and P. S. Masters.** Unpublished data.
61. **Rottier, P., J. Armstrong, and D. I. Meyer.** 1985. Signal recognition particle-dependent insertion of coronavirus E1, an intracellular membrane glycoprotein. J. Biol. Chem. **260:**4648–4652.
62. **Rottier, P. J. M.** 1995. The coronavirus membrane protein, p. 115–139. *In* S. G. Siddell (ed.), The Coronaviridae. Plenum Press, New York, N.Y.
63. **Rottier, P. J. M., M. C. Horzinek, and B. A. M. van der Zeijst.** 1981. Viral protein synthesis in mouse hepatitis virus strain A59-infected cells: effect of tunicamycin. J. Virol. **40:**350–357.
64. **Rottier, P. J. M., J. Krijnse Locker, M. C. Horzinek, and W. J. M. Spaan.** 1990. Expression of MHV-A59 M glycoprotein: effects of deletions on membrane integration and intracellular transport. Adv. Exp. Med. Biol. **276:**127–135.
65. **Rottier, P. J. M., and J. K. Rose.** 1987. Coronavirus E1 glycoprotein expressed from cloned cDNA localizes in the Golgi region. J. Virol. **61:**2042–2045.
66. **Siddell, S. G.** 1995. The small-membrane protein, p. 181–189. *In* S. G. Siddell (ed.), The Coronaviridae. Plenum Press, New York, N.Y.
67. **Simon, K., V. R. Lingappa, and D. Ganem.** 1988. Secreted hepatitis B surface antigen polypeptides are derived from a transmembrane precursor. J. Cell Biol. **107:**2163–2168.
68. **Simpson, D. A., and R. A. Lamb.** 1992. Alterations to influenza virus hemagglutinin cytoplasmic tail modulate virus infectivity. J. Virol. **66:**790–803.
69. **Stern, D. F., and B. M. Sefton.** 1982. Coronavirus proteins: structure and function of the oligosaccharides of the avian infectious bronchitis virus glycoproteins. J. Virol. **44:**804–812.
70. **Sturman, L. S., K. V. Holmes, and J. Behnke.** 1980. Isolation of coronavirus envelope glycoproteins and interaction with the viral nucleocapsid. J. Virol. **33:**449–462.
71. **Suomalainen, M., P. Liljeström, and H. Garoff.** 1992. Spike protein-nucleocapsid interactions drive the budding of alphaviruses. J. Virol. **66:**4737–4747.
72. **Tooze, S. A., J. Tooze, and G. Warren.** 1988. Site of addition of N-acetylgalactosamine to the E1 glycoprotein of mouse hepatitis virus-A59. J. Cell Biol. **106:**1475–1487.
73. **Vennema, H., G.-J. Godeke, J. W. A. Rossen, W. F. Voorhout, M. C. Horzinek, D.-J. E. Opstelten, and P. J. M. Rottier.** 1996. Nucleocapsid-independent assembly of coronavirus-like particles by co-expression of viral envelope protein genes. EMBO J. **15:**2020–2028.
74. **Vennema, H., R. Rijnbrand, L. Heijnen, M. C. Horzinek, and W. J. Spaan.** 1991. Enhancement of the vaccinia virus/phage T7 RNA polymerase expression system using encephalomyocarditis virus 5′-untranslated region sequences. Gene **108:**201–209.
75. **Wege, H., H. Wege, K. Nagashima, and V. ter Meulen.** 1979. Structural polypeptides of the murine coronavirus JHM. J. Gen. Virol. **42:**37–47.
76. **Whitt, M. A., L. Chong, and J. K. Rose.** 1989. Glycoprotein cytoplasmic domain sequences required for rescue of a vesicular stomatitis virus glycoprotein mutant. J. Virol. **63:**3569–3578.
77. **Yu, X., X. Yuan, M. F. McLane, T.-H. Lee, and M. Essex.** 1993. Mutations in the cytoplasmic domain of human immunodeficiency virus type 1 transmembrane protein impair the incorporation of Env proteins into mature virions. J. Virol. **67:**213–221.
78. **Zhao, H., B. Lindqvist, H. Garoff, C.-H. von Bonsdorff, and P. Liljeström.** 1994. A tyrosine-based motif in the cytoplasmic domain of the alphavirus envelope protein is essential for budding. EMBO J. **13:**4204–4211.
79. **Zoller, M. J., and M. Smith.** 1982. Oligonucleotide-directed mutagenesis using M13-derived vectors: an efficient and general procedure for the production of point mutations in any fragment of DNA. Nucleic Acids Res. **10:**6487–6500.